Journal of Sound and Vibration (1998) **210**(1), 91–115

LOCALIZATION OF DAMAGED STRUCTURAL CONNECTIONS BASED ON EXPERIMENTAL MODAL AND SENSITIVITY ANALYSIS

H. F. Lam, J. M. Ko and C. W. Wong

Department of Civil and Structural Engineering, The Hong Kong Polytechnic University, Hung Hom, Kowloon, Hong Kong

(*Received* 20 *March* 1997, *and in final form* 29 *August* 1997)

A method for the detection of damage location for framed structures has been proposed. Unlike most of the existing methods, the proposed method has been proven by a series of experimental case studies and found to be practical in real applications. This paper reports the theoretical development of the proposed method, and the verification of the method with one numerical case study by using a six-storey frame and one experimental case study by using a two-storey frame. Two techniques have been developed in this proposed method: the Approximate Parameter Change (APC) technique and the Damage Signature Matching (DSM) technique. Both techniques employ measured modal data before and after the structure is damaged. The combination of these two techniques forms a practical method for the detection of damage locations.

1. INTRODUCTION

The detection of damage occurrence based on a vibration measurement approach is direct and has been developed for many years [1–5]. The calculation of damage extent in terms of changes in the structures, physical parameters is not a difficult task, provided that the damage location is determined in advance. Many existing parameter identification techniques can be applied [6, 7]. As a result, many researchers have paid more attention to the identification of damage location.

Initially, a number of researchers tried to locate the damage using measured natural frequencies, as the measurement technique was not good enough to identify the mode shapes with acceptable accuracy, e.g, Cawley and Adams [8] in 1979, and Hearn and Testa [9] in 1991. This is due to the fact that the information provided by natural frequencies is insufficient; it is not unusual to locate the damage incorrectly when just using natural frequencies, especially when only the first few natural frequencies are obtained. For symmetrical structures, the changes in natural frequency due to damage at symmetric locations are exactly the same, and thus the damage location cannot be identified by using natural frequencies.

As mode shapes can provide much more information than natural frequency, many researchers have devoted their efforts to the area of damage detection with mode shape information, e.g, West [10] in 1986, Lieven and Ewins [11] in 1988, and Biswas *et al*. [12] in 1989. However, those methods cannot solve the problem with insufficient measured modal data (caused by missing d.o.f. in the measured modal vectors when compared with the theoretical modal vectors, and the lack of information from higher modes), and measurement error.

0022–460X/98/060091 + 25 $25.00/0/sv971302

A method, which is theoretically sound, may not be practical in reality. Furthermore, a method, which can detect a crack on a simple beam, may not be workable in damage detection for other structures. The method proposed in this paper is not only theoretically sound, but has also been experimentally verified as workable in framed structures, which are not as simple as a beam.

Based on recent developments in measurement and data analysis techniques, natural frequencies and mode shapes of the structural system can easily be obtained through an ambient vibration model test. The interference with the normal operation of the structure that results from taking measurements can be greatly reduced. Therefore, the new damage detection method has been developed on the basis of the available measured and analytical natural frequencies and mode shapes of the structural system.

Two techniques are developed in this proposed method, they are the Approximate Parameter Change (APC) technique and the Damage Signature Matching (DSM) technique. The APC technique can locate the damage by calculating the approximate change of system parameters based on two sets of modal data, which are measured before and after the structure is damaged. Owing to the approximate sense of this method and the existence of measurement error, the DSM technique was developed as a supplement to the APC technique for some complicated cases. Based on the same sets of modal data, measured damage signatures are determined. Predicted damage signatures for different possible damage locations are determined with reference to the mathematical model. The damage and its location on the structure can then be indicated from the pattern matching between the measured and predicted damage signatures.

Most of the existing damage detection methods concentrate on damage along members of the structure and neglect the damage at its connections, which in framed structures does in fact occur more frequently. Owing to its importance, both numerical and experimental verifications in this paper will focus on the detection of damage location at connections in the structure.

2. THEORETICAL DEVELOPMENT

2.1. APPROXIMATE PARAMETER CHANGE (APC) TECHNIQUE

Damage would alter system parameters, such as stiffness and mass of the structure [13]. In computer simulation, it can be represented by a reduction in value of the corresponding system parameters. When the system parameters corresponding to all possible damages are defined, the change in a system parameter can then be used as a means to detect the damage type and location. The exact change of system parameters is not required, if only the damage location is of primary interest.

To locate the changed system parameters, the relationship between the measured modal parameters and the system parameters must be derived. In general, any structural system can be represented by a N d.o.f. system. Assume that there are q possible damages in a structure, and the corresponding system parameters are $p_1, p_2, \dots, p_q$. The ith mode shape of the damaged structural system can be expressed as a function of these q system parameters and the relationship can be written in the form of a Taylor series expansion:

$$\{\phi_i\{\mathbf{p}\} + \Delta\{\mathbf{p}\})\} = \{\phi_i(\{\mathbf{p}\})\} + \sum_{j=1}^{q} \frac{\partial\{\phi_i\}}{\partial p_j} \Delta p_j + \sum_{j=1}^{q} \frac{\partial^2\{\phi_i\}}{\partial p_j^2} \Delta p_j^2 + \cdots, \tag{1}$$

where $\{\mathbf{p}\} = \{p_1, p_2, \dots, p_j, \dots, p_q\}^T$ is a vector of system parameters corresponding to all possible damages for the undamaged structure; $\Delta\{\mathbf{p}\}$ is a vector of changes in system parameters due to damage; $\{\phi_i(\{\mathbf{p}\})\}$ is the ith mode shape, as a function of system parameters, of the undamaged structural system; $\{\phi_i(\{\mathbf{p}\} + \Delta\{\mathbf{p}\})\}$ is the ith mode shape, as a function of system parameters, of the damaged structural system.

By neglecting higher order terms of $\Delta\{\mathbf{p}\}$, equation (1) can be expressed in matrix form as:

$$\Delta\{\phi_i\} \cong \left[\frac{\partial\{\phi_i\}}{\partial\{\mathbf{p}\}}\right]_{N \times q} \Delta\{\mathbf{p}\}_{p \times 1}, \tag{2}$$

where $\Delta\{\phi_i\} = \{\phi_i(\{\mathbf{p}\}) + \Delta\{\mathbf{p}\})\} - \{\phi_i(\{\mathbf{p}\})\}$ is the change in mode shape for mode i due to damage; $[\partial\{\phi_i\}/\partial\{p\}] = [\partial\{\phi_i\}/\partial p_1 \cdots \partial\{\phi_i\}/\partial p_q]$ contains the rates of change of mode shape for mode i with respect to system parameters corresponding to all q possible damages.

Equation (2) shows the relationship between the changes in modal vectors and the change in system parameters. Damage is a very local effect of a structure and natural frequency is a global parameter. It is not good practice to use a global parameter in the detection of damage. As a result, the proposed method will use the measured mode shapes, but not the natural frequency, in the detection of damage.

By means of the least-square method, the APC values for the ith mode can be estimated. For the number of equations equal to the number of unknowns ($N = q$):

$$\{\mathrm{APC}_i\} = \left[\frac{\partial\{\phi_i\}}{\partial\{\mathbf{p}\}}\right]^{-1} \Delta\{\phi_i\}. \tag{3}$$

For the number of equations greater than the number of unknowns ($N > q$):

$$\{\mathrm{APC}_i\} = \left(\left[\frac{\partial\{\phi_i\}}{\partial\{\mathbf{p}\}}\right]^T \left[\frac{\partial\{\phi_i\}}{\partial\{\mathbf{p}\}}\right]\right)^{-1} \left[\frac{\partial\{\phi_i\}}{\partial\{\mathbf{p}\}}\right]^T \Delta\{\phi_i\}. \tag{4}$$

For the number of equations smaller than the number of unknowns ($N < q$):

$$\{\mathrm{APC}_i\} = \left[\frac{\partial\{\phi_i\}}{\partial\{\mathbf{p}\}}\right]^T \left(\left[\frac{\partial\{\phi_i\}}{\partial\{\mathbf{p}\}}\right]\left[\frac{\partial\{\phi_i\}}{\partial\{\mathbf{p}\}}\right]^T\right)^{-1} \Delta\{\phi_i\}. \tag{5}$$

As damage reduces the value of system parameters, such as member stiffness, all the APC values with a comparatively large negative magnitude can be used as an indicator for the identification of the damages. If the damage indicated in all correlated modes is the same, it can be concluded with great confidence that it is the right damage case. In some cases, the damage case indicated in some correlated modes may be unclear owing to missing sensitive d.o.f., lack of higher modes information, measurement and modelling errors. In such instances, all possible damage cases have to be identified and the DSM technique will be used to pick up the most possible damage case.

It must be noted that equation (2) is only an approximation; the accuracy of the calculated system parameter changes decreases with increases in damage severity. Nevertheless, the damage can still be located once the changed system parameters are identified.

2.2. DAMAGE SIGNATURE MATCHING (DSM) TECHNIQUE

The magnitude of dynamic characteristic changes due to damage depends on both the damage severity and location. For a linear system and given damage location, the higher the damage severity, the larger the changes in the modal parameter will be. For a given damage severity, the damage at different locations will change the natural frequencies in different ways [8, 9], having a strong effect on certain modes and a weak effect on others. In the case of mode shapes, the effects of damage on different d.o.f. are also different. Therefore, if the effect of damage severity is eliminated, the values of all dynamic characteristic changes due to damage can be used as an indicator of the location of that damage.

If the changes in the dynamic characteristics for all possible damage cases are predicted with an analytical model, the measured dynamic characteristic changes can be compared with the predicted changes due to all possible damage cases. The set of predicted changes, which are well matched with the measured values, can be identified and the corresponding damage case can be considered as the damage of the structure. If this approach is used to detect the damage location, the effect of damage severity on the changes in modal parameters must first be eliminated. To solve this problem, the governing equation of free vibration for a damaged structure with N d.o.f. is considered:

$$[\mathbf{K} - \Delta\mathbf{K} - (\omega_j^2 - \Delta\omega_j^2)\mathbf{M}](\{\phi_j) - \Delta\{\phi_j\}) = 0, \tag{6}$$

where $\mathbf{K}$ and $\mathbf{M}$ are the system stiffness and mass matrices of the undamaged structure; ω_j and $\{\phi_j\}$ are the modal values and vectors of the undamaged structure; $\Delta\mathbf{K}$ is the change in system stiffness matrix due to damage; $\Delta\omega_j^2$ is the change in modal value of mode j due to damage; $\Delta\{\phi_j\}$ is the change in modal vector of mode j due to damage.

For civil engineering structures, damage resulting from the loss of structural components seldom exists. Therefore, it is reasonable to assume that the mass of the structure has no change, and the damage would alter only the stiffness matrix of the system. As a result, there is no $\Delta\mathbf{M}$ term in equation (6). After expansion and neglecting higher order terms of Δ, equation (6) becomes:

$$-[\Delta\mathbf{K} - \Delta\omega_j^2\mathbf{M}]\{\phi_j\} - [\mathbf{K} - \omega_j^2\mathbf{M}]\Delta\{\phi_j\} = 0. \tag{7}$$

To find an expression for changes in the modal values, pre-multiply equation (7) with $\{\phi_j\}^T$ and use the relationship $\{\phi_j\}^T\,[\mathbf{K} - \omega_j^2\mathbf{M}] = 0$, which gives the following equation:

$$\{\phi_j\}^T\Delta\mathbf{K}\{\phi_j\} - \Delta\omega_j^2\{\phi_j\}^T\mathbf{M}\{\phi_j\} = 0. \tag{8}$$

After rearranging, equation (8) can be written as:

$$\Delta\omega_j^2 = \frac{\{\phi\}^T\Delta\mathbf{K}\{\phi_j\}}{\{\phi\}^T\mathbf{M}\{\phi_j\}}\,. \tag{9}$$

Equation (9) is the expression of changes in the modal value of mode j. To find an expression for changes in the modal vectors, pre-multiply equation (7) with $\{\phi_s\}^T$ and use the relationship $\{\phi_s\}^T\mathbf{K} = \omega_s^2\{\phi_s\}^T\mathbf{M}$:

$$(\omega_s^2 - \omega_i^2)\{\phi_s\}^T\mathbf{M}\Delta\{\phi_i\} = -\{\phi_s\}^T\Delta\mathbf{K}\{\phi_i\}. \tag{10}$$

Since the mode shapes form a complete set of vectors, any N-component vector can be represented as a linear combination of the mode shapes [14]. Therefore, it is reasonable to assume:

$$\Delta\{\phi_i\} = \sum_{k=1}^{N} c_{ik}\{\phi_k\}, \tag{11}$$

where c_{ik} is the linear combination coefficient for the kth mode in the calculation of the change in mode shape of the ith mode.

Substitute equation (11) into equation (10):

$$(\omega_s^2-\omega_i^2)\{\phi_s\}^T\mathbf{M}\left(\sum_{k=1}^{V}c_{ik}\{\phi_k\}\right)=-\{\phi_s\}^T\Delta\mathbf{K}\{\phi_i\}. \tag{12}$$

Owing to the orthogonal property, equation (12) becomes:

$$(\omega_s^2-\omega_i^2)c_{is}\{\phi_s\}^T\mathbf{M}\{\phi_s\}=-\{\phi_s\}^T\Delta\mathbf{K}\{\phi_i\}. \tag{13}$$

After rearranging, equation (13) can be written as:

$$c_{is}=\frac{-\{\phi_s\}^T\Delta\mathbf{K}\{\phi_i\}}{(\omega_s^2-\omega_i^2)\{\phi_s\}^T\mathbf{M}\{\phi_s\}}. \tag{14}$$

Substitute equation (14) into equation (11), and the result is the expression of changes in modal vectors of mode i:

$$\Delta\{\phi_i\}=\sum_{s=1}^{N}\frac{-\{\phi_s\}^T\Delta\{\phi_i\}}{(\omega_s^2-\omega_i^2)\{\phi_s\}^T\mathbf{M}\{\phi_s\}}\{\phi_s\}. \tag{15}$$

Equations (9) and (15) give the expression of changes in modal values and vectors respectively.

The system stiffness matrix can be expressed as the summation of individual member stiffness matrices.

$$\mathbf{K}=\sum_{e=1}^{E}k_e, \tag{16}$$

where k_e is the individual member stiffness matrix expanded to the size of the system matrix; E is the number of elements in the model.

Similarly, changes in the stiffness matrix due to damage can be expressed as:

$$\Delta\mathbf{K}=\sum_{e=1}^{E_d}\Delta k_e, \tag{17}$$

where Δk_e is the change in the individual member stiffness matrix; E_d is the number of damaged members.

The change in individual stiffness of the member can be represented as a fractional change in the stiffness of the member. Therefore:

$$\Delta\mathbf{K}=\sum_{e=1}^{E_d}\alpha_e k_e. \tag{18}$$

where α_e is a scalar representing the fractional change in member stiffness.

For structures with single damage or multiple damages with similar severity, the scalar α_e can be extracted from the equation and represented as α. The changes in the modal vector of mode i divided by the changes in the modal value of mode j can be expressed as:

$$\frac{\Delta\{\phi_i\}}{\Delta\omega_j^2} = \frac{\displaystyle\sum_{s=1}^{N} \frac{-\{\phi_s\}^T \sum_{e=1}^{E_d} k_e \{\phi_i\}}{(\omega_s^2 - \omega_i^2)\{\phi_s\}^T \mathbf{M}\{\phi_s\}} \{\phi_s\}}{\dfrac{\{\phi_j\}^T \sum_{e=1}^{E_d} k_e \{\phi_j\}}{\{\phi_j\}^T \mathbf{M}\{\phi_j\}}}. \tag{19}$$

The scalar α used to denote damage extent is eliminated in the expression. As a result, equation (19) depends on damage location only, but not on extent. When the increment counter s is equal to i, the term is equal to zero. This can be proved by using the mass-orthonormal equation for the damaged structure:

$$(\{\phi_i\} - \Delta\{\phi_i\})^T(\mathbf{M} - \Delta\mathbf{M})(\{\phi_i\} - \Delta\{\phi_i\}) = 1. \tag{20}$$

After expansion and neglecting higher order terms of Δ, equation (20) can be written as:

$$1 + 2\{\phi_i\}^T\mathbf{M}\Delta\{\phi_i\} + \{\phi_i\}\Delta\mathbf{M}\{\phi_i\} = 1. \tag{21}$$

Assuming $\Delta\{\phi_i\} = \sum_{j=1}^{N} c_{ij}\{\phi_j\}$, equation (21) becomes:

$$2\{\phi_i\}^T\mathbf{M}\left(\sum_{j=1}^{N} c_{ij}\{\phi_j\}\right) = -\{\phi_i\}^T\Delta\mathbf{M}\{\phi_i\}. \tag{22}$$

Owing to the mass-orthonormal property, equation (22) can be written as:

$$c_{ii} = \frac{-\{\phi_i\}^T\Delta\mathbf{M}\{\phi_i\}}{2}. \tag{23}$$

As it is assumed that damage does not change the mass of the structure, c_{ii} is equal to zero. Therefore, when the increment counter s is equal to i, the term is equal to zero.

The ratio of changes in modal vector to changes in modal value is defined as the Damage Signature. The damage location can then be assessed by matching the Measured Damage Signatures (MDS) with the Predicted Damage Signatures (PDS) for different possible damage cases.

In the proposed method, the MDS of mode i is defined as the change in the measured modal vector of mode i divided by the change in the modal value of a reference mode, say mode 1:

$$\{\mathrm{MDS}_i\} = \frac{\Delta\{\phi_i\}}{\Delta\omega_1^2}. \tag{24}$$

The choice of the reference mode depends on two factors: the measurement accuracy of a mode, and the sensitivity of a mode with respect to the damage. As the sensitivity of a mode with respect to the damage is not known in advance and it is believed that the accuracy of the measured natural frequency of mode 1 is the highest, mode 1 is employed as reference mode in this paper. However, if the change in the natural frequency of the first mode is too small, another mode should be used as reference mode instead. It is because a very small denominator in equation (24) will cause numerical difficulty in the calculation of the MDS vector. Before the calculation of $\Delta\{\phi_i\}$, it must be ensured that the two sets of measured modal vectors have the same normalization.

Since the changes in any system parameter due to damage are not known in advance, it is impossible to calculate the PDS by equation (19). Thus, sensitivity analysis is employed in the PDS calculation. The use of sensitivity analysis is possible as:

$$\Delta\{\phi_i\} = \frac{\partial\{\phi_i\}}{\partial p_k}\Delta p_k, \tag{25}$$

and

$$\Delta\omega_1^2 = \frac{\partial w_1^2}{\partial p_k}\Delta p_k, \tag{26}$$

where $\partial\{\phi_i\}/\partial p_k$ is the rate of change of the modal vector for the ith mode with respect to the system parameter corresponding to the kth damage parameter; $\partial\omega_1^2/\partial p_k$ is the rate of change of the modal value for the 1st mode with respect to the system parameter corresponding to the kth damage parameter.

Therefore, the changes in the modal vector of mode i normalized with the change in the modal value of mode 1 can be calculated analytically as:

$$\{\mathrm{PDS}_{ik}\} = \frac{\Delta\{\phi_i\}}{\Delta\omega_1^2} = \frac{\dfrac{\partial\{\phi_i\}}{\partial p_k}\Delta p_k}{\dfrac{\partial\omega_1^2}{\partial p_k}\Delta p_k} = \frac{\dfrac{\partial\{\phi_i\}}{\partial p_k}}{\dfrac{\partial\omega_1^2}{\partial p_k}}. \tag{27}$$

For each possible damage location identified by APC technique, the corresponding predicted damage signatures are compared with the measured damage signatures. The damage can be located with full confidence, if there is possible damage for which the corresponding damage signatures are well matched for all available modes. Matching between measured and predicted damage signatures for different possible damages can be done by visual comparison, if the measured and predicted damage signatures are plotted against the number of measured d.o.f. Another more systematic way to match the damage signatures is to calculate the norm of difference between the predicted and the measured damage signature for each mode. The summation of the norms for all modes is defined as the total discrepancy for that possible damage case. The possible damage case with the smallest discrepancy is believed to be the actual damage on the structure. The formulation of total discrepancy can be written as:

$$D_k = \sum_{j=1}^{m} \|\{\mathrm{PDS}_{ik}\} - \{\mathrm{MDS}_i\}\|, \tag{28}$$

where D_k is the total discrepancy between the measured and the predicted damage signature for possible damage k.

TABLE 1

Sectional and material properties of the six-storey frame

	Column	Beam
Young's modulus (E)	$2{\cdot}00 \times 10^{11}$ N/m^2	$2{\cdot}00 \times 10^{11}$ N/m^2
Sectional area (A)	0·00298 m^2	0·0032 m^2
Moment of inertia (I)	0·0000126 m^4	0·0000236 m^4
Density (r)	8590 kg/m^3	7593 kg/m^3
Rotational stiffness at column–base connection		50×10^5 Nm/rad
Rotational stiffness at beam–column connection		30×10^5 Nm/rad

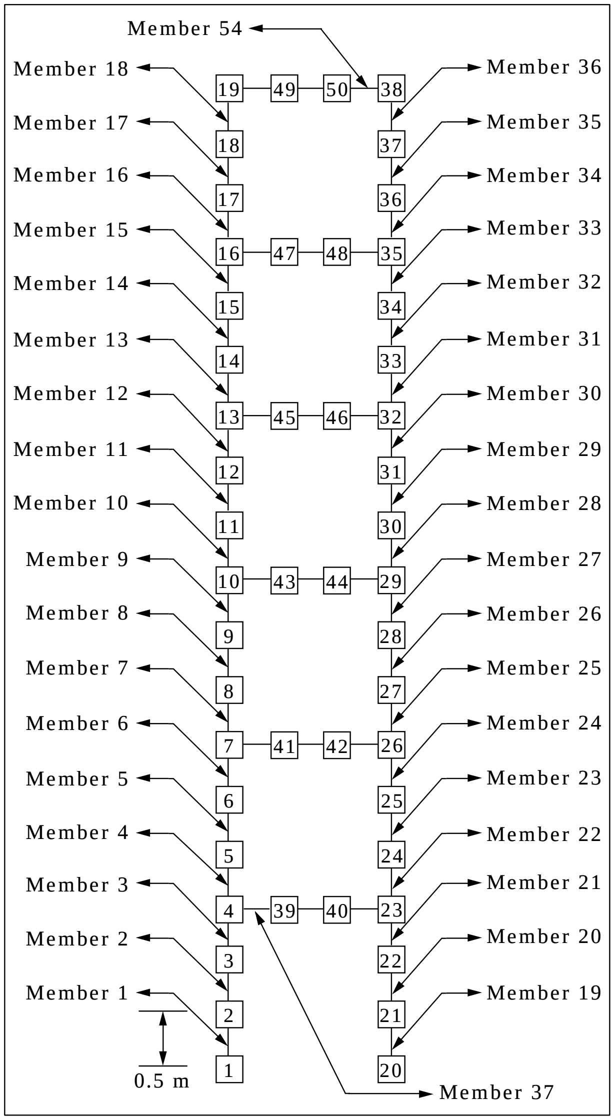

Figure 1. Modelling of the six-storey frame.

If all possible damages on the structure have to be considered, the time and computational cost for the calculation of PDS and matching is enormous. However, the number of considerable possible damages will be greatly reduced after the application of the APC technique. The successive application of both techniques forms a practical method for the detection of damage location.

3. CASE STUDIES

For most existing damage detection methods, the area of application is restricted in order to detect the damage on a member of a structure. This may be accomplished through reduction in the cross-sectional area and degradation of Young's modulus, but very few methods can deal with damage at a structural connection. However, this type of damage is very common for framed structures. As a single joint is usually connected to several beams and columns, the connected elements may make the joint inaccessible and methods such as visual inspection cannot be employed. It is obvious that a damage detection method which can handle damage at a connection is in demand. In order to demonstrate the ability of the proposed method, locating damages at structural connections is emphasized in both the numerical and experimental verifications.

3.1. NUMERICAL VERIFICATION

As a start, a mathematical model of a six-storey frame was used to verify the proposed method. The six-storey frame is built with standard 152 × 152 × 23-UC as columns and 203 × 133 × 25-UB as beams. Both the column-base and beam-column connections of the

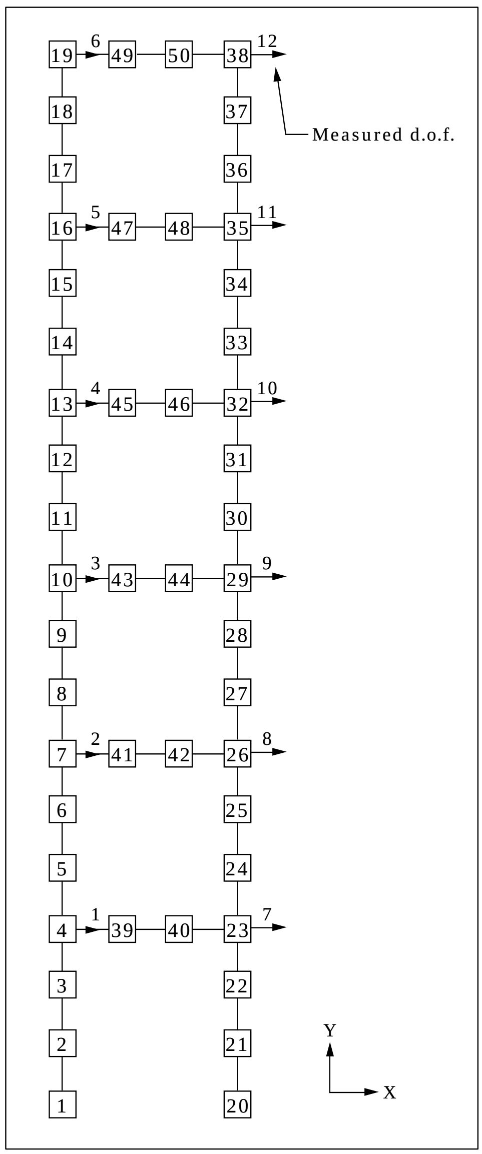

Figure 2. Numbering of d.o.f.

TABLE 2

MAC matrix for the undamaged and damaged structure

Undamaged/damaged	Mode 1	Mode 2	Mode 3	Mode 4
Mode 1	0·9999	0·0183	0·0168	0·0182
Mode 2	0·0136	0·9995	0·0254	0·0188
Mode 3	0·0186	0·0159	0·9992	0·0277
Mode 4	0·0169	0·0226	0·0168	0·9992

frame are treated as semi-rigid and the rotational stiffness used in the simulation is shown in Table 1. The sectional and material properties are also summarized in Table 1.

The frame is modelled by 54 standard two-dimensional frame elements with the same length and is composed of 50 nodes. The numbering of both members and nodes is given in Figure 1. Although the modal value and modal vector for all d.o.f. of each mode can be calculated, only the first four modes and 12 out of 144 d.o.f. were used in the present study to simulate incomplete modal data in the real situation. The measured d.o.f. are shown in Figure 2. The modal values and modal vectors (12 d.o.f.) for the first four modes were treated as measured modal parameters for the undamaged structure.

Damage was simulated at node 1 by reducing the rotational stiffness of spring element at that node from 50 to 25×10^5 Nm/rad. Another set of modal parameters was then calculated and treated as data for the damaged structure. The Modal Assurance Criterion (MAC) matrix [1, 4] for the undamaged and damaged structure was determined and is shown in Table 2. As a guideline, all mode pairs with a MAC value higher than 0·9 will be treated as correlated, so that the first four modes are all correlated.

All possible damages and the corresponding system parameters must be defined. As only damage at the connection is considered, the number of possible damages equals the

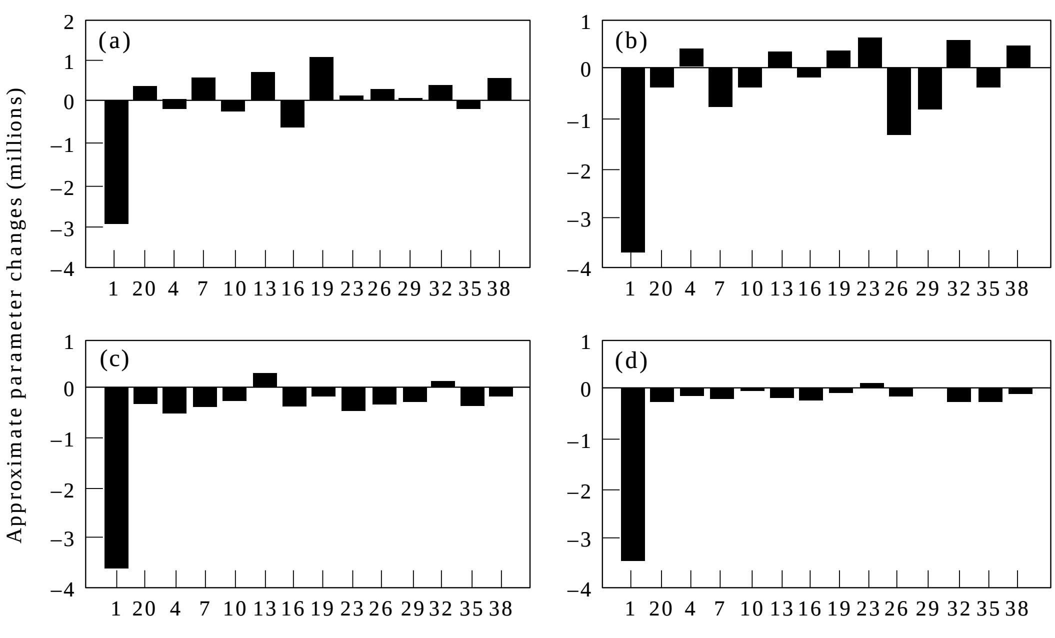

Figure 3. APC values for: (a) CM1, (b) CM2; (c) CM3; (d) CM4.

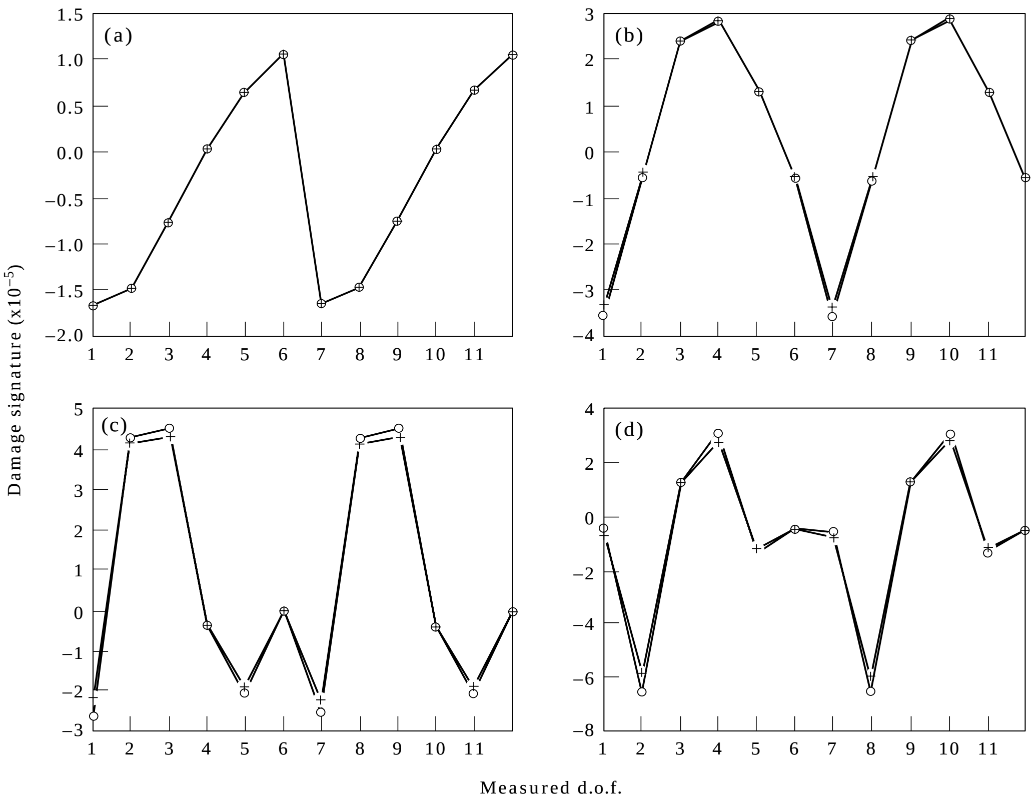

Figure 4. Matching of MDS with PDS for damage at node 1. (a) CM1; (b) CM2; (c) CM3; (d) CM4. +, Measured; ○, predicted.

number of connections of the structure. For the frame under consideration, 14 possible damage locations have to be considered and the corresponding system parameter is the rotational stiffness of each spring element.

As the number of unknowns (= 14) was larger than the number of equations (= 12), equation (5) was used. For each correlated mode, the APC values for all possible damages were calculated and are shown in Figures 3(a–d), respectively. In these figures, it is clearly demonstrated that the damage is at node 1 of the frame. As all the correlated modes show the same result, it is undoubtedly clear that the damage was correctly located. In this case, it is not necessary to apply the DSM technique.

Although the damage can be located without the application of the DSM technique, the measured and predicted damage signatures for damage at node 1 (right damage location) and node 7 (wrong damage location) were plotted in Figures 4(a–d) to illustrate the function of the DSM technique. It is very clear that the matching between the measured damage signatures and the rightly predicted damage signatures is excellent for all four correlated modes, but the matching is very poor for the wrongly predicted damage signatures.

The total discrepancy for damage at node 1 (right damage location) is $1{\cdot}7 \times 10^{-5}$ and that for damage at node 7 (wrong damage) is $2{\cdot}7 \times 10^{-4}$. Therefore, both visual comparison and total discrepancy calculation show that the damage is more likely at node 1. This numerical verification shows the ability of both APC and DSM techniques in the detection of damage location.

3.2. EXPERIMENTAL VERIFICATION

To verify the proposed method in a laboratory situation, experiments on a two-storey steel frame were carried out. The elevation of the two-storey steel frame is shown in Figure 6. It was modelled by 18 two-dimensional frame elements of equal length. The numbering of nodes and elements are shown in Figure 7. The columns and beams of the frame are constructed by standard 127×76 and 152×76 joists sections respectively. The detailing of beam–column and column–base connections are shown in Figures 8 and 9, respectively.

For this kind of beam–column connection, the initial rotational stiffness in static cases is about 30×10^5 Nm/rad [15]. For convenience, this value was used in the modelling of both beam–column and column–base connections. The appearance of beam–column and column–base connections are shown in Figures 10 and 11, respectively.

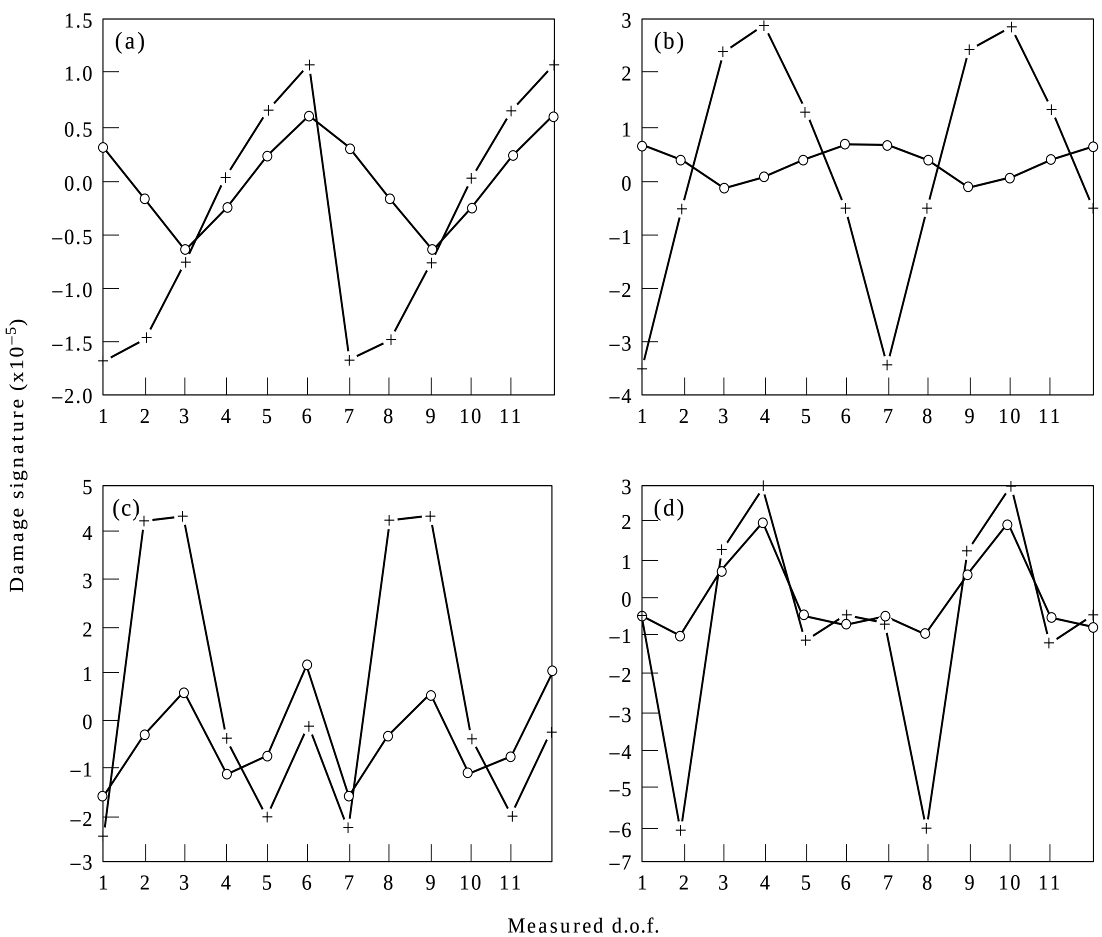

Figure 5. Matching of MDS with PDS for damage at node 7. (a) CM1; (b) CM2; (c) CM3; (d) CM4. +, Measured; ○, predicted.

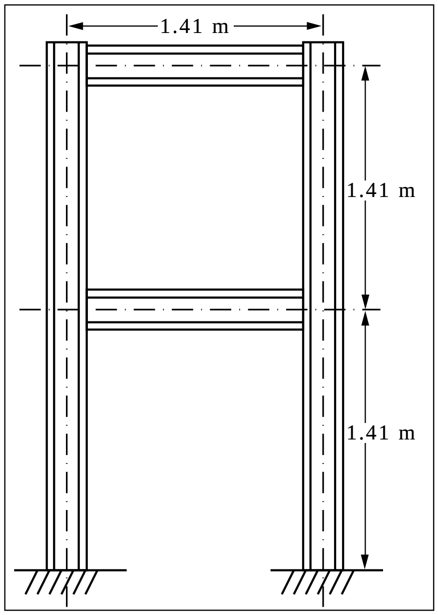

Figure 6. Elevation of frame.

An impact hammer [16] was used as a means for exciting the frame (Figure 12). A force transducer (B and K type) was used to pick up the force applied on the structure, and accelerometers (B and K type) were employed to obtain the responses of the structure. All the signals (applied force and responses) were sent to the Dynamic Test and Analysis System (DTAS) [17], which consists of data acquisition and signal processing hardware for further processing. Both the time and frequency domain information (frequency response function) were then transferred from the DTAS to a PC equipped with Dynamic

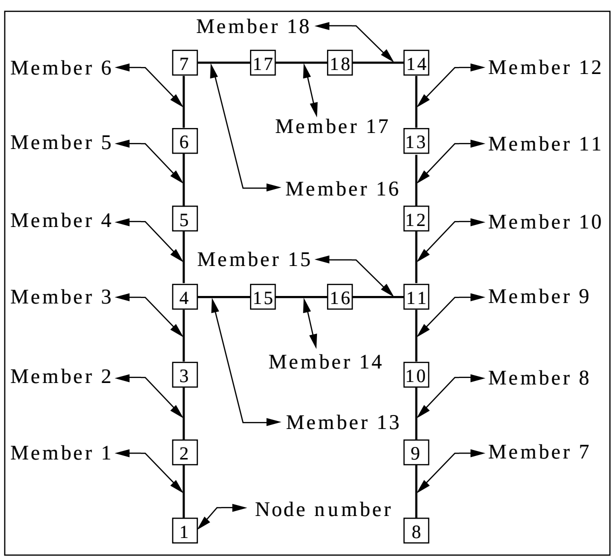

Figure 7. Modelling of frame.

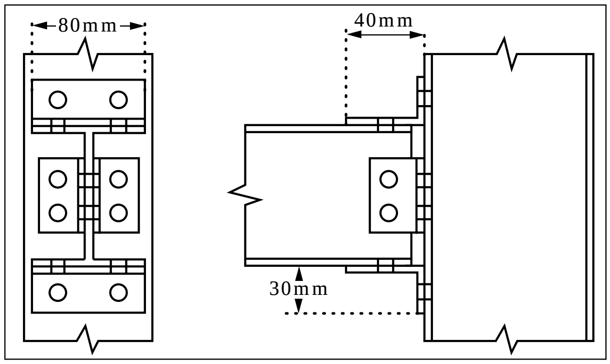

Figure 8. Beam–column connection details.

Signal Analysis (DSA) software [18]. Modal parameters such as natural frequency and mode shape could then be easily determined using software Structural Modal Analysis (MODAL) [19].

Before commencement of the experimental work, the degree of tightness of the bolts at each connection was checked using a torque wedge. This procedure is done to ensure that the axial force of all bolts are approximately identical. Initially, the axial force of each bolt was maintained at about 30 kN.

Various damage events were simulated on the frame [20], but only three of them are presented here. The three events are summarized in Table 3. Except for the damage in case D4b, all damages were simulated by removing both the top and seat angles of the connection. For the damage in case D4b, only the top angle was removed in order to simulate damage to a smaller extent.

Before the structure was damaged, a set of natural frequencies and mode shapes was measured and treated as the reference modal data. Different damage cases were then simulated on the structure separately. For each damage case, one set of modal data was measured. For the columns, only the horizontal d.o.f. were measured and for the beams, only the vertical d.o.f. were measured.

3.2.1. *Damage case D4a*

For this case, a single damage was simulated at node 4 (beam–column connection) of the two-storey frame. For estimation of the correlated modes, the MAC matrix for theoretical and experimental modes was worked out and is shown in Table 4. The mode pairs with MAC values greater than 0·9 are treated as correlated mode pairs. From this

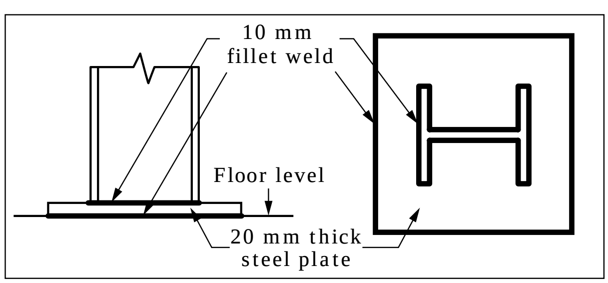

Figure 9. Column–base connection details.

Figure 10. Beam–column connection.

table, it is found that theoretical modes 1, 2, 3, 4, 5 and 10 are correlated to experimental modes 1, 2, 3, 4, 5 and 9, respectively. The MAC matrix for the undamaged and damaged structure is shown in Table 5, and indicates that modes 1, 2, 3, 4 and 9 of the undamaged structure are correlated to modes 1, 2, 3, 4 and 9 of the damaged structure, respectively.

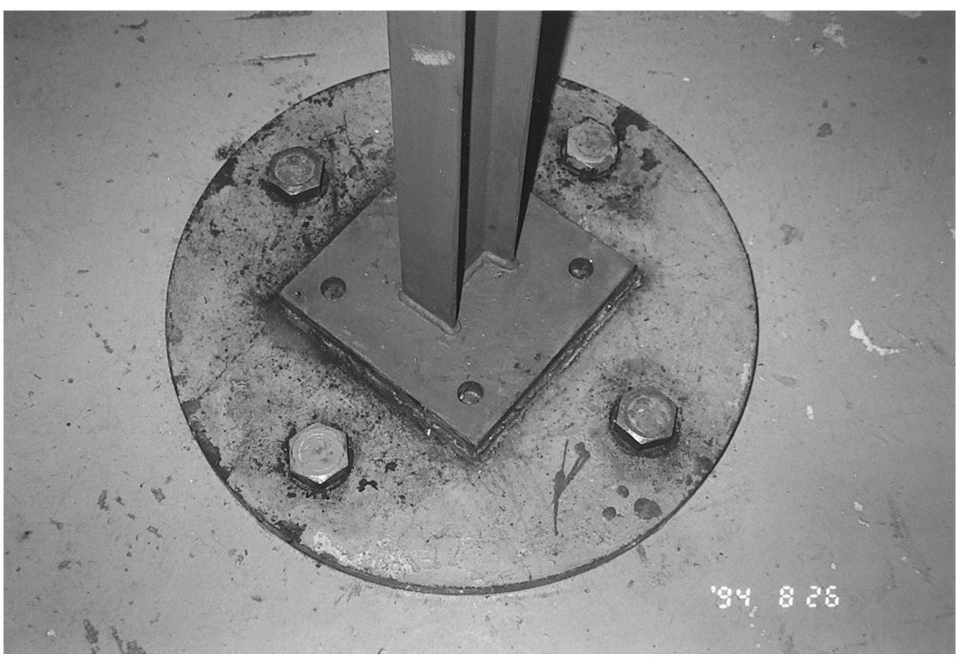

Figure 11. Column–base connection.

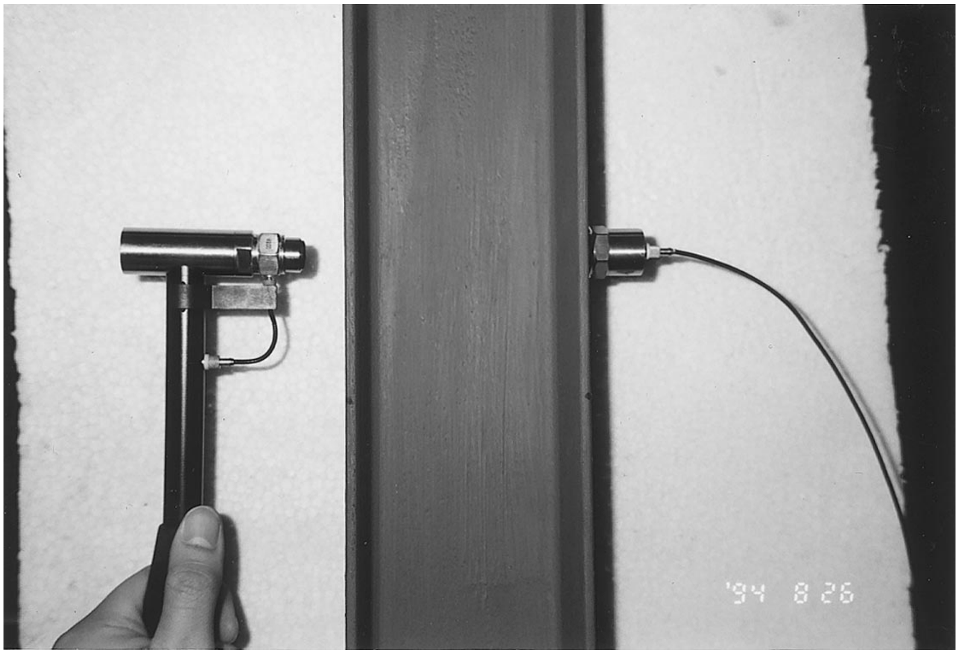

Figure 12. Impact hammer and accelerometer used in testing.

Based on the information provided by both tables, the correlated modes could be identified and are listed in Table 6.

Figures 13(a–f) show the APC values for all six correlated modes. Results from all correlated modes indicate that the damage was at node 4, and therefore, the APC technique can locate the damage at node 4. As the damage is clearly located by the APC technique, it is not necessary to use the DSM technique in this case.

3.2.2. *Damage case D4b*

The damage location in this case was the same as that of the previous damage case, but it was simulated in a different way. Only the top angle of the connection was removed not the seat angle. The damage severity in this case is clearly smaller than that of the previous damage case.

After the determination of correlated modes, APC values for all possible damages were calculated and plotted in Figures 14(a–f). Results from all the correlated modes show that the damage was at node 4.

Apart from node 4, the APC values for node 11 in correlated modes 1, 2, 3, 5 and 6 are negative. Although the APC value for node 11 is positive for correlated mode 4, it is however so small that node 11 could still reasonably be considered as a possible damage

Table 3

Different damage cases for the two-storey steel frame

Number	Damage case	Damage description
1	D4a	Damage at node 4
2	D4b	Smaller damage at node 4
3	D4 and 11	Damage at nodes 4 and 11

TABLE 4

MAC matrix for theoretical and experimental mode shapes

Theory/ experimental	1	2	3	4	5	6	7	8	9
1	0·9998	0·0122	0·0001	0·0000	0·0150	0·0034	0·0013	0·1080	0·0017
2	0·0034	0·9965	0·0001	0·0000	0·0334	0·0065	0·0001	0·0321	0·0000
3	0·0000	0·0002	0·9845	0·0745	0·0023	0·0003	0·0005	0·0070	0·0105
4	0·0000	0·0000	0·0013	0·9294	0·0322	0·2003	0·0103	0·0006	0·4277
5	0·0188	0·0239	0·0013	0·0065	0·9191	0·1291	0·0003	0·0000	0·0005
6	0·0000	0·0000	0·0004	0·0017	0·0495	0·7512	0·8168	0·0121	0·2725
7	0·0000	0·0000	0·0043	0·0025	0·0004	0·0032	0·0231	0·0830	0·0025
8	0·1081	0·0414	0·0003	0·0018	0·0108	0·0073	0·0351	0·7311	0·0193
9	0·1095	0·0510	0·0001	0·0001	0·0072	0·0004	0·0004	0·8828	0·0012
10	0·0000	0·0000	0·0379	0·5555	0·0015	0·0120	0·3882	0·0011	0·9324

location. Consequently, damage may occur solely at node 4 or it may occur both at nodes 4 and 11. The DSM technique has to be used to identify the most possible case.

Measured and predicted damage signatures for damage at node 4 were plotted in Figures 15(a–f) while damage at nodes 4 and 11 were plotted in Figures 16(a–f). The matching based on visual comparison is very subjective and not very reliable so total discrepancy for both damage cases were calculated. The total discrepancy for damage at node 4 was $6{\cdot}8 \times 10^{-5}$, which is smaller than $9{\cdot}0 \times 10^{-5}$ which was found for damage at both nodes 4 and 11. Therefore, the DSM technique located the damage at node 4.

Although the APC value cannot give the exact extent of the damage, it can, to some degree, be used to indicate the relative severity of the damage. To illustrate this, the calculated APC values for damage case D4a (large damage severity) and D4b (small damage severity) are summarized in Table 7. The column D4a/D4b shows the ratio of APC values of damage case D4a to that of D4b.

Apart from correlated mode 6, all APC values for case D4a are greater than those for case D4b. The exception round in the case of correlated mode 6 may be caused by measurement error. Based upon the average of APC values for all correlated modes, the APC value for large damage severity is $-7{\cdot}64 \times 10^{6}$ Nm/rad and that for small damage severity is $-5{\cdot}04 \times 10^{6}$ Nm/rad. Therefore the damage extent for case D4a is 1·52 times that for case D4b. The value 1·52 is reasonable.

TABLE 5

MAC matrix for undamaged and damaged structure (D4a)

Undamaged/ damaged	1	2	3	4	5	6	7	8	9
1	0·9982	0·0176	0·0001	0·0001	0·0114	0·0085	0·0006	0·1276	0·0021
2	0·0074	0·9987	0·0007	0·0003	0·0267	0·0013	0·0003	0·0370	0·0002
3	0·0000	0·0002	0·9700	0·0588	0·0166	0·0017	0·0009	0·0021	0·0228
4	0·0001	0·0000	0·0077	0·9759	0·0128	0·1115	0·0477	0·0040	0·4892
5	0·0235	0·0330	0·0118	0·0040	0·9397	0·0054	0·0223	0·0000	0·0012
6	0·0043	0·0069	0·0069	0·1043	0·0012	0·9870	0·4548	0·0103	0·0415
7	0·0020	0·0001	0·0060	0·0467	0·0504	0·4691	0·7845	0·0535	0·3452
8	0·1037	0·0378	0·0075	0·0014	0·0013	0·0002	0·0068	0·9827	0·0076
9	0·0008	0·0001	0·0585	0·4793	0·0001	0·0706	0·3839	0·0008	0·9409

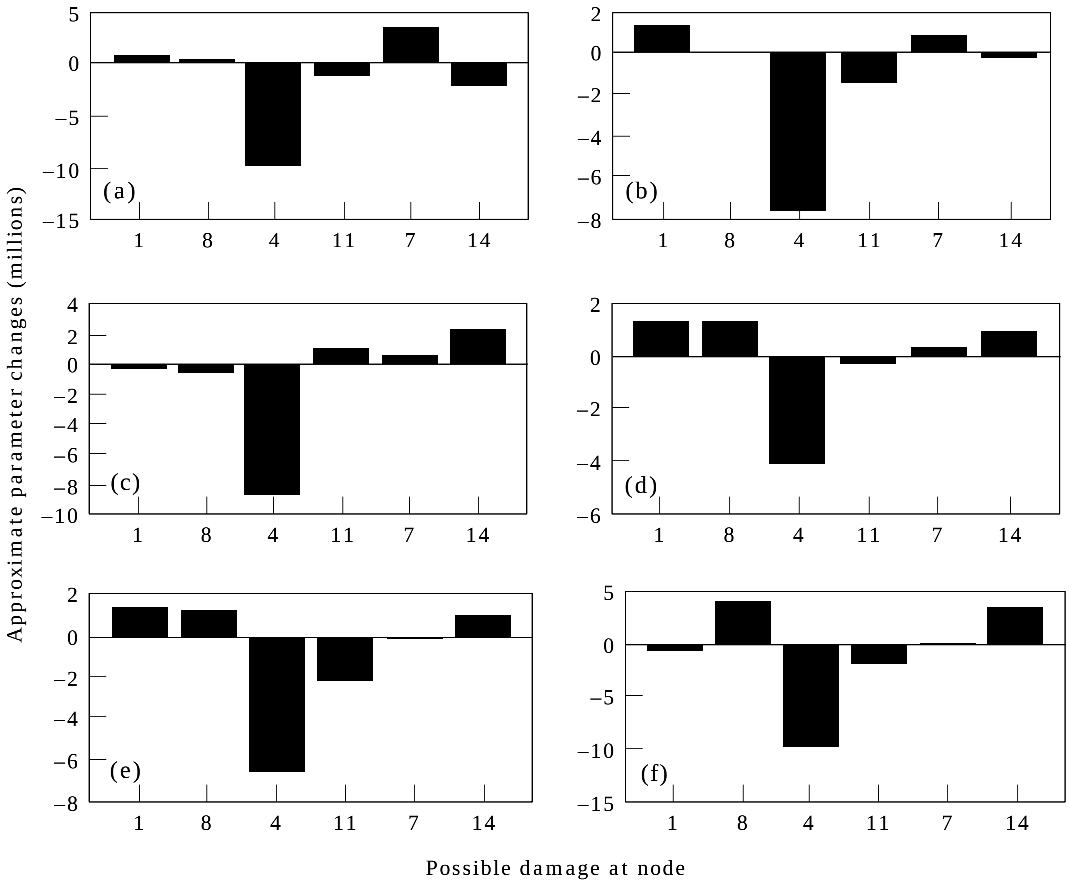

Figure 13. APC values for: (a) CM 1 (D4a); (b) CM 2 (D4a); (c) CM 3 (D4a); (d) CM 4 (D4a); (e) CM 5 (D4a); (f) CM 6 (D4a).

Verification with the first two damage cases proves the proposed method gives very satisfactory results when there is only one damaged connection in the structure. If more correlated modes are available in the investigation, the damage can be located with greater confidence as there are more cross references. In the next section, the application of the proposed method in dealing with more than one damaged connection in the structure is reported.

TABLE 6

Number of correlated modes (D4a)

Correlated mode	Theoretical	Experimental	
		Undamaged	Damaged
1	1	1	1
2	2	2	2
3	3	3	3
4	4	4	4
5	5	5	5
6	10	9	9

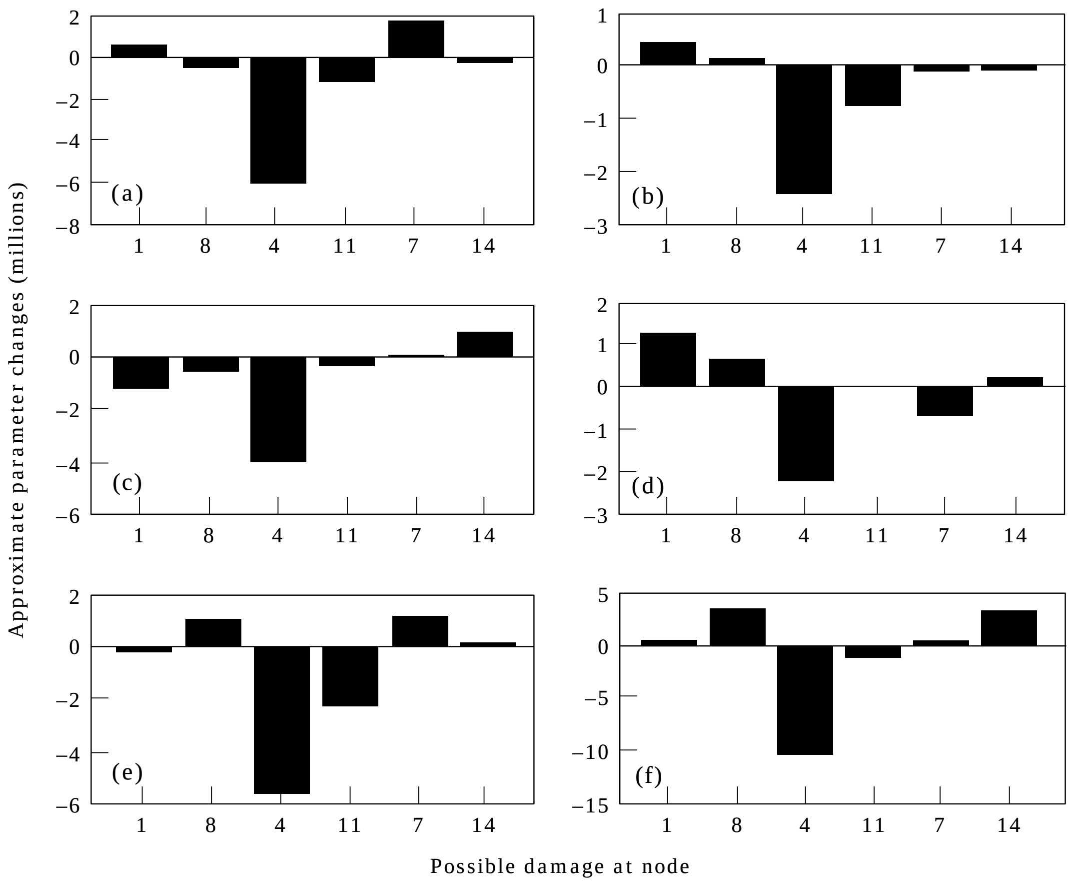

Figure 14. APC values for: (a) CM 1 (D4b); (b) CM 2 (D4b); (c) CM 3 (D4b); (d) CM 4 (D4b); (e) CM 5 (D4b); (f) CM 6 (D4b).

3.2.3. *Damage case D*4 *and* 11

In this case, damage was simulated at nodes 4 and 11. The same procedures were carried out as before. Five correlated modes were identified from theoretical and experimental results. APC values for all possible damages of each correlated mode were worked out and were plotted in Figures 17(a–e).

From all the correlated modes, the APC values at nodes 4 and 11 are comparatively large and are very close to each other. As a result, the APC technique locates the damages at nodes 4 and 11. As the indication of damage locations is very clear, the DSM technique is not necessary.

4. DISCUSSIONS

In both the numerical and experimental verifications, damage at the connections are emphasized. This type of damage can be simulated by the reduction of rotational stiffness of the spring element modelled at the damaged connection. Damage along a member, such as material degrading, can be simulated by reducing Young's modulus and the proposed method can be applied to locate the damage by the same procedures as shown in the case studies.

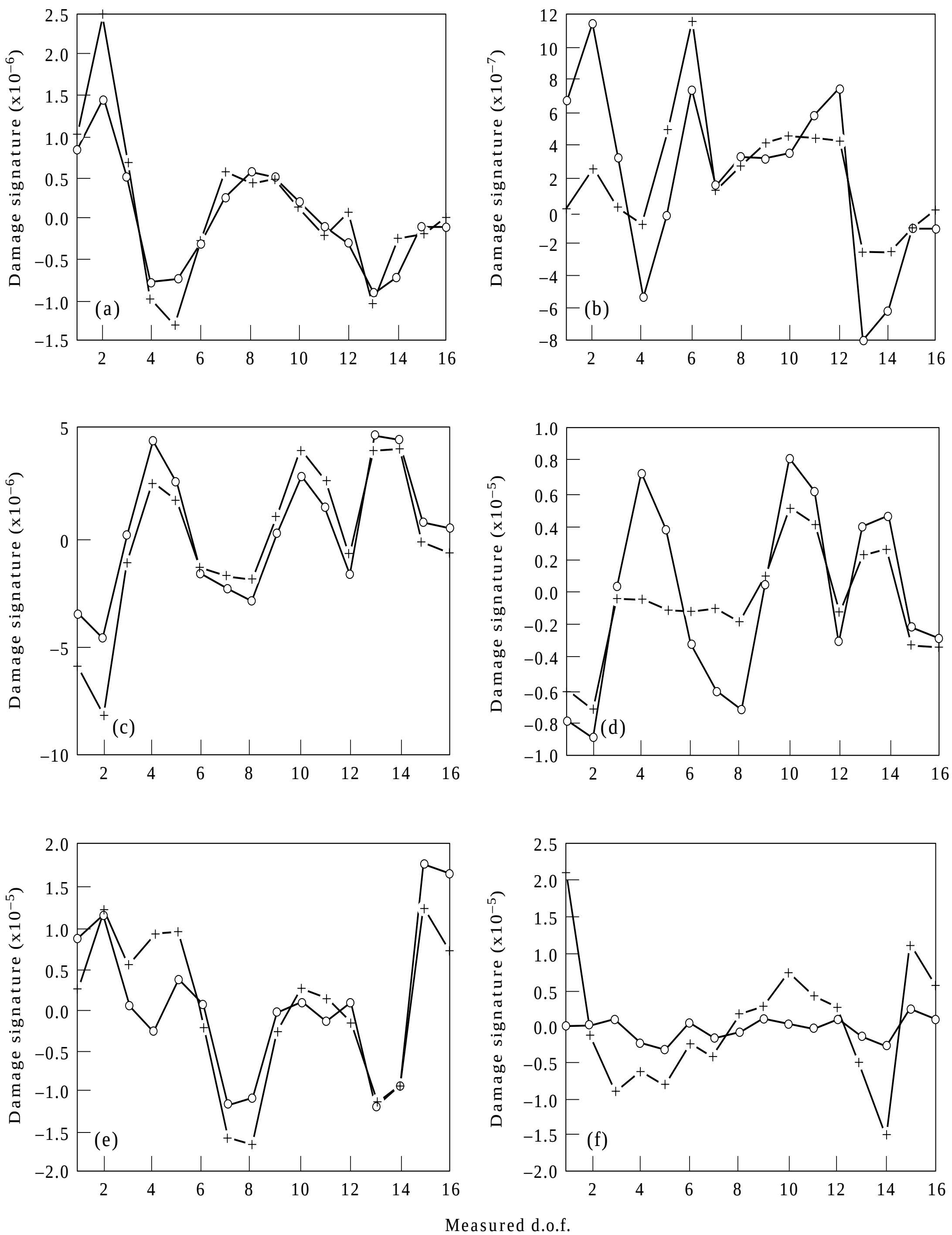

Figure 15. Damage at node 4. (a) CM 1; (b) CM 2; (c) CM 3; (d) CM 4; (e) CM 5; (f) CM 6. +, Measured; ○, predicted.

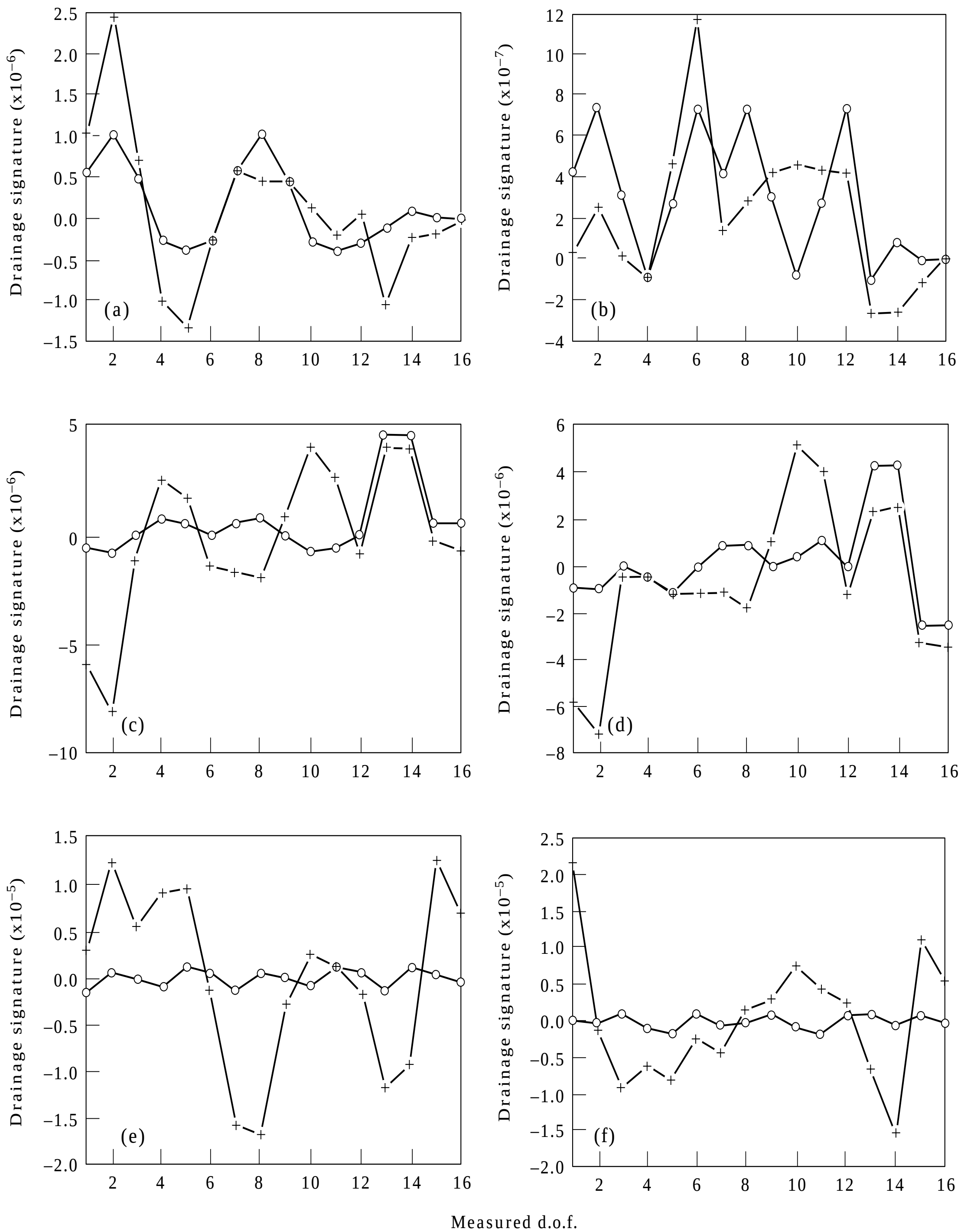

Figure 16. Damage at nodes 4 and 11. (a) CM 1; (b) CM 2; (c) CM 3; (d) CM 4; (e) CM 5; (f) CM 6. +, Measured; ○, predicted.

TABLE 7

APC values for damage at node 4 with different damage severity

Correlated modes	APC for D4a ($\times 10^6$ Nm/rad)	APC for D4b ($\times 10^6$ Nm/rad)	D4a/D4b
1	−9·44	−5·96	1·58
2	−7·51	−2·38	3·16
3	−8·68	−4·00	2·17
4	−4·11	−2·18	1·89
5	−6·46	−5·52	1·17
6	−9·65	−10·2	0·95
Average	−7·64	−5·04	1·52

It is worth pointing out that, if all types of damage were treated as possible damage on the structure, the number of possible damages would be very large. As each possible damage needs to have its own sensitivity analysis, increases in the number of possible damages will result in greater computational times and costs. In some cases, the MAC values and the change in natural frequencies after the structure is damaged can provide some idea about the type or the approximate region of damage. If it is recognized that,

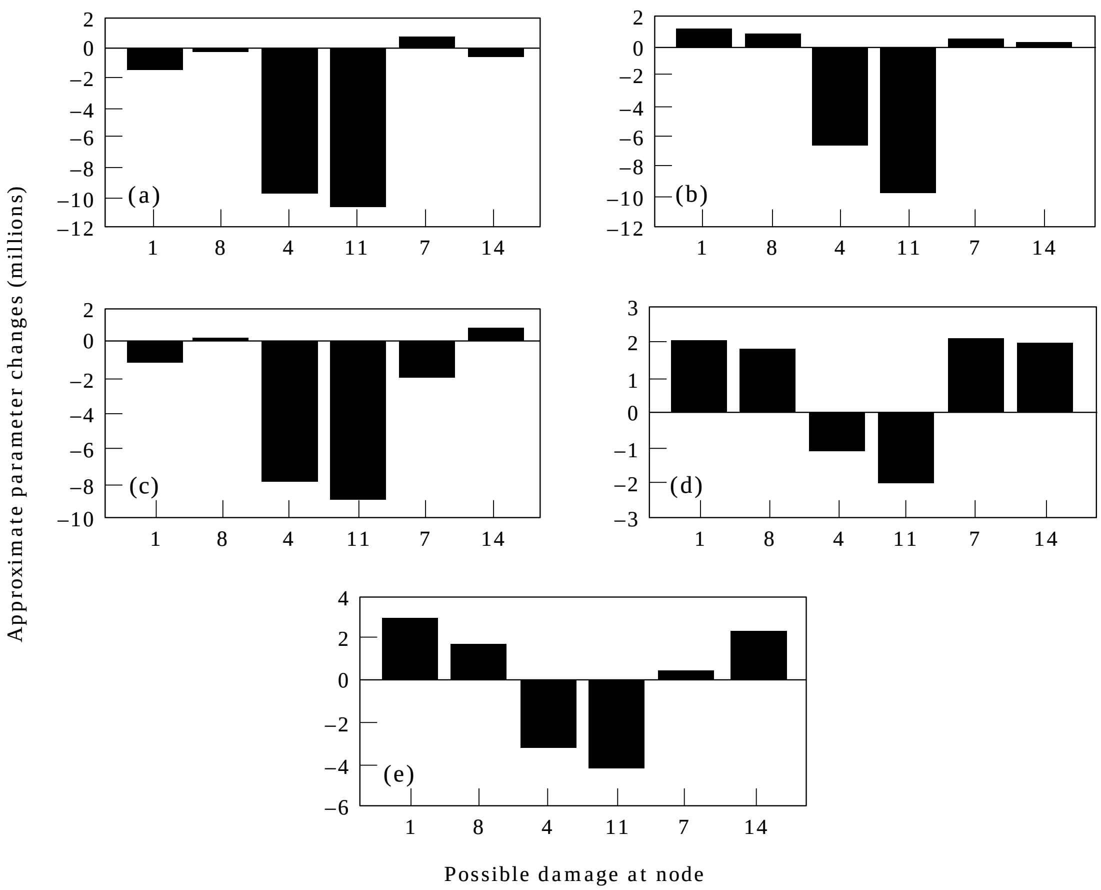

Figure 17. APC values for: (a) CM 1 (D4 and 11); (b) CM 2 (D4 and 11); (c) CM 3 (D4 and 11); (d) CM 4 (D4 and 11); (e) CM 5 (D4 and 11).

for some correlated modes, the MAC values are relatively low or the changes in natural frequencies are comparatively large, those modes must be more sensitive to the damage in comparison with other modes. In case all the sensitive modes are swaying modes, the damage is likely to be at the support connections. This is because the change in support conditions has a significant effect on the sway modes of the structure. In cases where all the sensitive modes are beam bending modes, the damage is more likely to be found at the beam–column connections, since the change of beam–column conditions has a significant effect on the capacity of transmitting bending moment from beam to column. Furthermore, in cases where all the sensitive modes are axial modes, the damage is likely to be a reduction of the members' axial stiffness, such as Young's modulus and cross-sectional area. If there are local modes, the location of possible damages can be declared even more easily.

5. CONCLUSIONS

The proposed method, which is based on sensitivity and experimental modal analysis, has been developed for the detection of damage locations for skeletal structures. The proposed method has been verified by numerical and experimental case studies with particular reference to steel-framed structures with damages at its connections. Upon verification, it can be concluded with full confidence that the proposed method is not only technically sound in computer simulation, but is also practical in real life situations. The proposed method provides a reliable indication of damage location, regardless of whether it is at a column–base or beam–column connection. It can also be applied to single damage locations as well as to multiple damage locations. As indicated in the computer simulation, it has been demonstrated that the proposed method can be applied to large scale structures where the number of measured d.o.f. is much smaller than the d.o.f. of the mathematical model. Furthermore, although the APC values cannot represent the exact magnitude of damage, experimental verification demonstrates that the APC values, to some extent, show the relative damage severity.

REFERENCES

1. R. J. ALLEMANG and D. L. BROWN 1982 *Proceedings of the 1st International Modal Analysis Conference* **I**, 110–116. A correlation coefficient for modal vector analysis.
2. V. G. IDICHANDY and C. GANAPATHY 1990 *Experimental Mechanics* 382–391. Modal parameters for structural integrity monitoring of fixed offshore platforms.
3. H. J. SALANE and J. W. BALDWIN 1990 *Experimental Mechanics*, 109–113. Changes in modal parameters of a bridge during fatigue testing.
4. T. WOLFF and M. RICHARDSON 1989 *Proceedings of the 7th International Modal Analysis Conference*, 87–94. Fault detection in structures from changes in their modal parameters.
5. K. WYCKAERT, R. SNOEYS and P. SAS 1988 *Proceedings of the 5th International Modal Analysis Conference* **II**, 921–927. A feasibility study for the application of frequency monitoring techniques in quality control.
6. J. C. CHEN and J. A. GARBA 1980 *AIAA Journal* **18**, 684–690. Analytical model improvement using modal test results.
7. S. R. IBRAHIM and A. A. SAAFAN 1987 *Proceedings of the 5th International Modal Analysis Conference* **II**, 1651–1660. Correlation of analysis and test in modeling of structures assessment and review.
8. P. CAWLEY and R. D. ADAMS 1979 *Journal of Strain Analysis* **14**, 49–57. The location of defects in structures from measurements of natural frequencies.
9. G. HEARN and R. B. TESTA 1991 *Journal of Structural Engineering* **117**, 3042–3063. Modal analysis for damage detection in structures.

10. W. M. West 1986 *Proceedings of the* 4*th International Modal Analysis Conference* **I**, 1–5. Illustration of the use of modal assurance criterion to detect structural changes in an orbiter test specimen.
11. N. A. J. Lieven and D. J. Ewins 1988 *Proceedings of the* 5*th International Modal Analysis Conference* **I**, 690–695. Spatial correlation of mode shapes, the coordinate modal assurance criterion (comac).
12. M. Biswas, A. K. Pandey and M. M. Samman 1989 *The International Journal of Analytical and Experimental Modal Analysis* **5**, 33–42. Diagnostic experimental spectral/modal analysis of a highway bridge.
13. C. Spyrakos, H. L. Chen, J. Stephens and V. Govindaraj 1990 *Proceedings of International Workshop on Intelligent Structures*, *Taipei*, *Taiwan*, 137–154. Evaluating structural deterioration using dynamic response characterization.
14. R. L. Fox and M. P. Kapoor 1968 *AIAA Journal* **6**, 2426–2429. Rates of change of eigenvalues and eigenvectors.
15. A. Azizinamini, J. H. Bradburn and J. B. Radziminski 1987 *Journal of Construction and Steel Research* **8**, 71–90. Initial stiffness of semi-rigid steel beam-to-column connection.
16. D. J. Ewins 1986 *Modal Testing*: *Theory and Practice*. New York: Wiley. See ch. 3, 102–104.
17. The Nanjing University of Aeronautics & Astronautics. 1992 *Dynamic Test and Analysis System Measurement Hardware Service Manual*: first edition.
18. The Nanjing University of Aeronautics & Astronautics. 1992 *Dynamic Test and Analysis System DTAS-DSA V1.2 User Manual*: first edition.
19. The Nanjing University of Aeronautics & Astronautics 1988 *Dynamic Test and Analysis System NAI-MODAL User Manual*: first edition.
20. H. F. Lam 1994 *Mphil*. *thesis*, *The Hong Kong Polytechnic University*. Detection of damage location based on sensitivity & experimental modal analysis.

APPENDIX: NOTATION

$\{\mathbf{p}\}$	$=\{p_1, p_2, \ldots, p_j, \ldots, p_q\}^T$, is a set of system parameters corresponding to all possible damages for the undamaged structure
$\Delta\{\mathbf{p}\}$	changes in system parameters due to damage
$\{\phi_i(\{\mathbf{p}\})\}$	mode shape of mode i for the undamaged structural system, as a function of system parameters
$\Delta\{\phi_i\}$	$=\{\phi_i(\{\mathbf{p}\}+\Delta\{\mathbf{p}\})\}-\{\phi_i(\{\mathbf{p}\})\}$, is the change in mode shape for mode i due to damage
$[\partial\{\phi_i\}/\partial\{\mathbf{p}\}]$	$=[\partial\{\phi_i\}/\partial p_1, \ldots, \partial\{\phi_i\}/\partial p_q]$, contains the rates of change of mode shape for mode i with respect to system parameters corresponding to all q possible damages
$\Delta\omega_i$	change in measured natural frequency for mode i due to damage
$[\partial\omega_i/\partial\{\mathbf{p}\}]$	$=[\partial\omega_i/\partial p_1, \partial\omega_i/\partial p_2, \ldots, \partial\omega_i/\partial p_i, \ldots, \partial\omega_i/\partial p_q]$, contains the rates of change of natural frequency for mode i with respect to different affected system parameters
$\mathbf{K}$, $\mathbf{M}$	system stiffness and mass matrices of the undamaged structure
ω_j, $\{\phi_j\}$	modal values and vectors of the undamaged structure
$\Delta\mathbf{K}$	changes in system stiffness matrix due to damage
$\Delta\omega_j^2$	changes in natural frequency of mode j due to damage
$\Delta\{\phi_j\}$	changes in mode shape of mode j due to damage
c_{ik}	linear combination coefficient for the kth mode in the calculation of the change in mode shape of the ith mode
k_e	individual member stiffness matrix expanded to the size of the system matrix by fitting with zero
E	number of elements in the model
Δk_e	change of individual member stiffness matrix
E_d	number of damaged member
α_e	a scalar representing the fractional change in member stiffness
$\partial\{\phi_i\}/\partial p_k$	rate of change of modal vector for mode i with respect to the system parameter corresponding to the kth possible damage
$\partial\omega_1^2/\partial p_k$	rate of change of modal value for mode i with respect to the system parameter corresponding to the kth possible damage
D_k	total discrepancy between measured and predicted damage signature for possible damage k

$\{APC_i\}$	Approximate Parameter Change values for the ith mode
$\{MDS_i\}$	Measured Damage Signatures of mode i
$\{PDS_{ik}\}$	Predicted Damage Signatures of mode i for the kth possible damage
MAC	Modal Assurance Criterion